

# Kondo effect in a few-electron quantum ring

U. F. Keyser,\* C. Fühner, S. Borck, and R. J. Haug

*Institut für Festkörperphysik, Universität Hannover, Appelstr. 2, 30167 Hannover, Germany*

M. Bichler and G. Abstreiter

*Walter Schottky Institut, TU München, 85748 Garching, Germany*

W. Wegscheider

*Angewandte und Experimentelle Physik, Universität Regensburg, 93040 Regensburg, Germany*

(Dated: December 2, 2024)

A small quantum ring with less than 10 electrons was studied by transport spectroscopy. For strong coupling to the leads a Kondo effect is observed and used to characterize the spin structure of the system in a wide range of magnetic fields. At small magnetic fields Aharonov-Bohm oscillations influenced by Coulomb interaction appear. They exhibit phase jumps by  $\pi$  at the Coulomb-blockade resonances. Inside Coulomb-blockade valleys the Aharonov-Bohm oscillations can also be studied due to the finite conductance caused by the Kondo effect. Astonishingly, the maxima of the oscillations show linear shifts with magnetic field and gate voltage.

PACS numbers: 72.15.Qm, 73.21.La, 73.23.Hk, 73.40.Gk

The characterization of semiconductor quantum dots by transport spectroscopy turned out to be an extremely successful approach to understand the physics of interacting electrons confined to a quasi-zero dimensional potential well [1]. Until recently the only accessible shape of these quantum dots was a tiny disc or box with a simple topology. With new fabrication techniques it is now possible to create more complex, multiple connected topologies, namely small quantum rings with an outer and an *inner* boundary. These novel devices combine characteristics of classical quantum dots with electronic interference phenomena like the Aharonov-Bohm effect [2]. Their properties are modulated periodically with the magnetic flux threading the ring.

First small quantum rings were fabricated by self-assembled growth of InAs on GaAs [3, 4], but these structures were mainly used for optical experiments. An alternative approach, the local oxidation of GaAs/AlGaAs-heterostructures with an atomic force microscope (AFM) [5], allows to directly write tuneable quantum rings into a two-dimensional electron gas [6, 7]. These rings can be studied by tunneling experiments. Due to their small size, transport is dominated by Coulomb blockade [1] and the number of electrons on such a ring can be controlled by an external gate voltage. Recently, Führer *et al.* studied a quantum ring containing a few hundred electrons in this regime [6]. Their measurements showed an Aharonov-Bohm effect and allowed to deduce the energy spectra [8] of their device. It turned out that their system can be well described within a single-particle picture [6] because of an effective screening of the electron-electron interaction by a metallic top gate.

Here we discuss a small quantum ring containing less than ten electrons in a totally different regime. Due to the lack of a screening top gate the ground state of our ring is dominated by strong electron-electron interactions. These interactions are predicted to cause frequent level crossings

because of a lifted degeneracy between singlet and triplet states [9], apparent as a smaller Aharonov-Bohm period compared to the noninteracting case. In our ring, we find indeed such a reduction of the Aharonov-Bohm period. Additionally, a strong coupling of the AFM-fabricated device to the leads allows us to investigate a Kondo effect [10] in our small quantum ring. This well known many-body phenomenon describes the formation of a spin singlet between electrons on ring and leads [11, 12]. It has attracted great interest in conventional, disc-shaped quantum dots [13, 14, 15, 16]. The finite Kondo conductance allows us to study the Aharonov-Bohm interference effects even in Coulomb-blockade valleys. We report a smooth shift of the Aharonov-Bohm oscillations with magnetic field and gate voltage and compare it to recent results for a quantum dot embedded into one arm of an Aharonov-Bohm ring [17, 18].

We fabricated our quantum ring from a  $\delta$ -doped GaAs/AlGaAs-heterostructure containing a two-dimensional electron gas (2DEG) 34 nm below the surface. Details on the layer structure can be found in Ref. [7]. The 2DEG has an electron density of  $n_e \sim 4 \cdot 10^{15} \text{ m}^{-2}$  and a mobility  $\mu_e \sim 50 \text{ m}^2 \text{V}^{-1} \text{s}^{-1}$  at low temperatures. After the fabrication of Hall bars the devices are mounted into an AFM for local oxidation with a conducting tip. Underneath the oxide the 2DEG is depleted [5]. By applying high oxidation currents we are able to create insulating regions in the 2DEG and write complex structures directly into the electronic system with an accuracy better than 10 nm. More details on our fabrication scheme can be found in Ref. [19].

An AFM-image of the completed ring structure is shown in Fig. 1(a). The two in-plane gates *A* and *B* are separated from the ring by the rough oxide lines. The ring is connected to the leads by two 150 nm wide point contacts. Both point contacts are tuned by gate *A* whereas

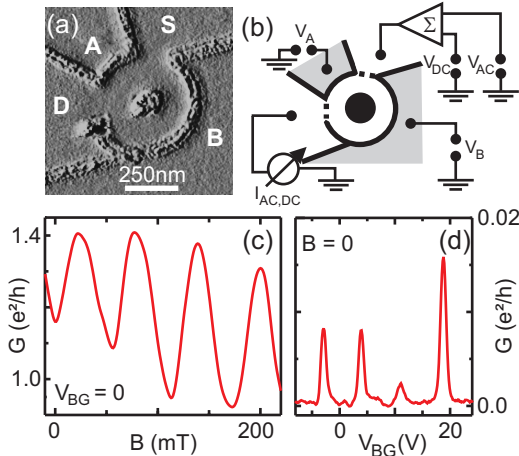


FIG. 1: (a) AFM image of the quantum ring.  $A, B$  denote the in-plane gates,  $S$  and  $D$  the source and drain contacts. The inner diameter of the ring is 190 nm and the outer 450 nm. (b) Scheme of our measurement setup. (c) Aharonov-Bohm oscillations in the open regime of the quantum ring ( $V_A, V_B > 0$  mV). (d) Coulomb-blockade oscillations as a function of the backgate voltage ( $V_A = -250$  mV,  $V_B = -100$  mV,  $B = 0$ ).

gate  $B$  couples only to the source contact. The inner diameter of the ring is 190 nm and the outer diameter 450 nm. In the following experiments, gate  $A$  is kept at a constant voltage  $V_A$ , and  $V_B$  is used to control the number of electrons on the ring. Our measurement setup is depicted in Fig. 1(b). All transport measurements were performed in a  $^3\text{He}/^4\text{He}$ -dilution refrigerator with an AC-excitation voltage of 5  $\mu\text{V}$  at 89 Hz, added to a variable DC-voltage  $V_{SD}$ . The base temperature during the experiments was  $T_b = 30$  mK. From the temperature dependence of the Coulomb-blockade peaks we deduce an effective temperature of less than 50 mK for the electronic system.

In the open transport regime with  $V_A, V_B \geq 0$  mV, we obtain an Aharonov-Bohm period  $\Delta B \sim 60$  mT for electrons that are transmitted ballistically in a perpendicular magnetic field. Fig. 1(c) shows an example of such a measurement. The observed periodicity corresponds to a diameter of 300 nm for the electronic orbit, which fits perfectly to the geometric values.

For measurements in the Coulomb-blockade regime we apply  $V_A, V_B < -50$  mV to separate the ring from the contacts by tunnelling barriers. Typical Coulomb-blockade oscillations as a function of the voltage  $V_{BG}$  applied to a metallic back gate are shown in Fig. 1(d). By analyzing Coulomb-blockade diamonds from nonlinear conductance measurements we extract a charging energy of  $U \sim 1.5$  meV and a single-particle level spacing of  $\delta E \sim 150$   $\mu\text{eV}$ .

The addition spectrum of our small quantum ring is shown in Fig. 2 for magnetic fields up to  $B = 6$  T. The linear conductance  $G$  ( $V_{SD} = 0$ ) is plotted in grey scale as function of  $V_B$  and  $B$  at  $V_A = -80$  mV. Each Coulomb-blockade peak appears as a black line more or less parallel to the  $B$ -axis. Signatures of non-vanishing con-

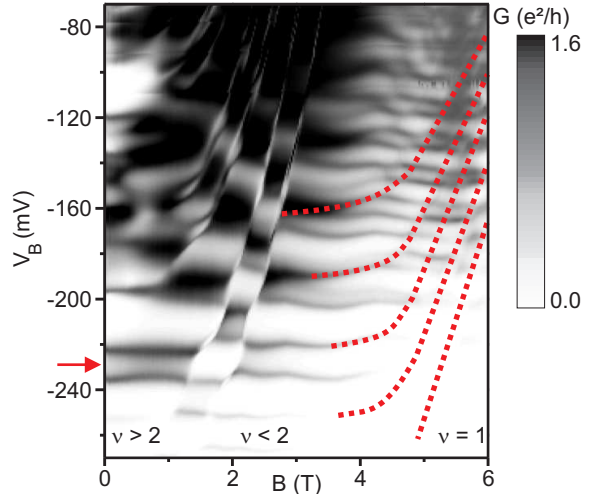


FIG. 2: Linear conductance  $G$  through the ring in function of the perpendicular magnetic field  $B$  and the gate voltage  $V_B$  at  $V_A = -80$  mV.

ductance between Coulomb-blockade peaks are observed and attributed to the Kondo effect, e. g. as marked by the arrow in Fig. 2. If electrons are added according to Hund's rule [20], a Kondo effect is expected in consecutive Coulomb-blockade valleys [21]. In contrast, we observe an alternation of the Kondo effect with electron number on the ring (odd-even Kondo effect [13]) below a gate voltage of -200 mV.

An alternating pattern of high and low conductance is also observed as a function of magnetic field. The Kondo effect is modulated abruptly between high (grey) and low (white) conductance regions for  $B < 2$  T. Interestingly, these results (Fig. 2) show some similarities with results obtained for quantum dots designed as discs [21, 22]. This is presumably due to the similar importance of the outer edge for tunneling through quantum dots as well as quantum rings in high magnetic fields. The alternating pattern of the valley conductance with magnetic field can be explained by a redistribution of electrons between different Landau levels (LL) [23]. For example, inside the valley marked in Fig. 2 we observe an increased conductance indicating a Kondo effect with an unpaired spin in the transport state at small magnetic fields. At  $B \sim 1.5$  T an electron from the upper LL is transferred to the lower LL which is indicated by the sharp boundary in the spectrum. The Kondo effect is suppressed because here the transport level in the lowest and outermost LL  $n = 0$  contains two electrons with opposite spins ( $N = \text{odd}$ , spin-0 in  $n = 0$ ). At  $B \sim 2.0$  T a second electron is transferred to LL  $n = 0$  and thus an unpaired spin is available again in LL  $n = 0$ . The Kondo effect is restored. For higher magnetic fields similar drastic changes are not observed anymore. We conclude that no further electrons are redistributed from LL  $n = 1$  to  $n = 0$  and therefore assume that all electrons are in the lowest Landau level (filling factor  $\nu = 2$ ).

With a further increase of the magnetic field up to  $B \sim$

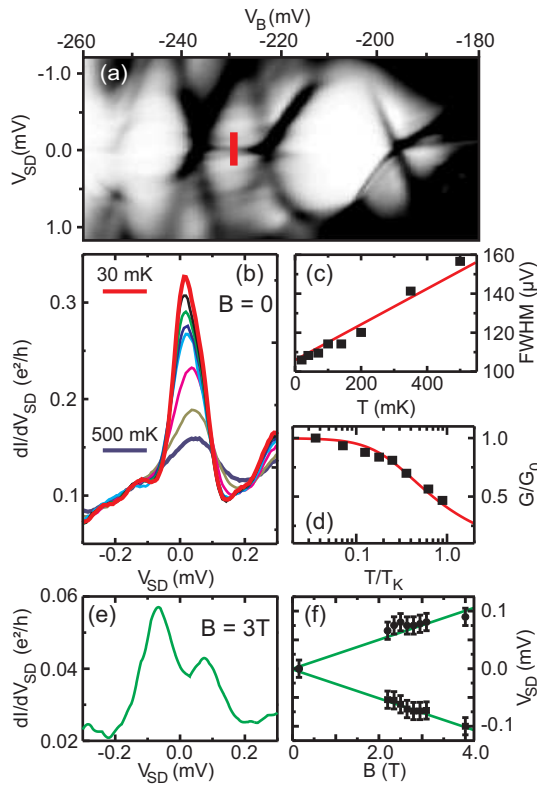


FIG. 3: (a) Grey scale plot of the differential conductance as function of  $V_B$  and source-drain voltage  $V_{SD}$  at  $V_A = -80$  mV and  $B = 0$  with black (white) high (low)  $G$ . (b) Temperature dependence of the zero-bias peak in the center of the  $N = 5$ -diamond (marked by the short bar in (a)),  $T=30, 50, 70, 100, 140, 200, 350, 500$  mK. (c) Temperature dependent full width at half maximum (FWHM). (d) Peak conductance scaled with  $T_K = 600$  mK and  $G_0 = 0.33e^2/h$ . (e) Split Kondo resonance at  $B = 3$  T. (f)  $B$ -dependent positions of the split peaks. The lines show the expected position for a Zeeman split spin-1/2 Kondo effect.

5.5 T we observe some weaker features highlighted in Fig. 2 by dashed lines. These small variations in the amplitude and position of the Coulomb-blockade peaks are identified with spin flips of the electrons in the lowest LL. Their spin is flipped from  $|\uparrow\rangle$  to  $|\downarrow\rangle$  by increasing the magnetic field [24]. For  $B > 5.5$  T, the electrons in the lowest LL are totally spin-polarized corresponding to a filling factor  $\nu = 1$ . The number of electrons  $N$  on the ring is determined by counting the spin flips between  $\nu = 2$  ( $B = 2$  T) and  $\nu = 1$  ( $B \sim 5.5$  T). For the marked Kondo valley, we observe only two spin flips. The occurrence of the Kondo effect at  $B = 0$  indicates that  $N$  is odd, thus we conclude that there are five electrons on the quantum ring. The same considerations apply for the surrounding Coulomb-blockade valleys, for which one extracts  $N = 4$  and  $N = 6$ , respectively.

To analyze this Kondo effect in more detail, non-linear transport measurements are shown in Fig. 3. Fig. 3(a) depicts the differential conductance  $dI_{SD}/dV_{SD}$  measured at a temperature of  $T_b = 30$  mK as function of  $V_B$  and  $V_{SD}$  ( $V_A = -80$  mV,  $B = 0$ ). The central Coulomb-blockade

diamond corresponds to the valley discussed above. A sharp zero-bias peak appears whereas in the valleys to the left and right only low conductance is observed. Fig. 3(b) depicts temperature dependent measurements at the gate voltage marked in Fig. 3(a). The zero-bias peak observed at  $T_b = 30$  mK vanishes almost completely when the temperature is increased to  $T \sim 500$  mK as expected for a Kondo resonance [25]. From these measurements we estimate a Kondo temperature  $T_K$  by extrapolation of the full peak width at half maximum  $\Delta V_{SD}$  to  $T = 0$  K (Fig. 3(c)), which results in  $T_K \approx e\Delta V_{SD,T=0}/2k_B \sim 600$  mK [25, 26]. In agreement, fitting the peak conductance at zero bias  $G(T)$  with an empirical formula from Ref. [26, 27],  $G(T) = G_0 / (1 + (2^{1/s} - 1)(T/T_K)^2)^s$  yields  $T_K \sim 600$  mK and  $s \sim 0.25$ . This is expected for a spin-1/2 system [27]. The scaled peak conductance is shown together with the fit in Fig. 3(d).

The zero-bias peak of a spin-1/2 Kondo effect is expected to split in a magnetic field according to the Zeeman effect,  $\Delta E = g_{GaAs}\mu_B B$  ( $g_{GaAs} = 0.44$ ,  $\mu_B$  Bohr's magneton). This peak splitting is shown at  $B = 3$  T in Fig. 3(e) in a nonlinear conductance measurement. The different peak amplitudes are related to a slight asymmetry in the coupling of the ring to the leads. The peak positions in  $V_{SD}$  extracted from several such measurements for  $2 \text{ T} < B < 4 \text{ T}$  are plotted in Fig. 3(f), the lines indicate the expected peak positions. We observe a nice agreement with the measurement for  $B > 2$  T which is another evidence for a spin-1/2 Kondo effect. Between 1.5 T and 2.1 T the Kondo effect is absent due to the paired spin configuration. For  $B < 1.5$  T the peak splitting is not resolved, presumably due to the broadening of the Kondo peak of the order of  $k_B T_K \sim 50 \mu\text{eV}$ .

The Coulomb-blockade peaks are broadened due to the strong coupling in the Kondo regime as well. This broadening obscures the small shifts in the peak positions as e.g. induced by changes of the ground states in the ring. To avoid this, the Kondo valley marked in Fig. 2 is shown again in Fig. 4(a) at a slightly lower tunnel coupling at  $V_A = -150$  mV. This reduces the conductance in the Kondo regime to below  $0.1(e^2/h)$ . Due to the finite capacitance between the ring and gate A, the valley is shifted to  $V_B \sim -185$  mV. In Fig. 4(b) we show Aharonov-Bohm oscillations in the normalized conductance  $G/G_0$  as a function of  $B$  for the gate voltages marked by the symbols in Fig. 4(a). The vertical dashed lines denote the expected period of  $\Delta B \sim 60$  mT of the Aharonov-Bohm oscillations extracted from the measurements in the open regime. It is immediately evident that we obtain a much *shorter* period. This shorter period is in contrast to the results of Fuhrer *et al.* [6], who obtained the *normal* Aharonov-Bohm period for their ring with many electrons and a front gate screening the electron-electron interaction.

Our shorter period has to be linked to our smaller electron number and their unscreened interaction. These fast oscillations are reflected by the movement of the Coulomb-blockade peaks in Fig. 4(c) as well. Each kink in the

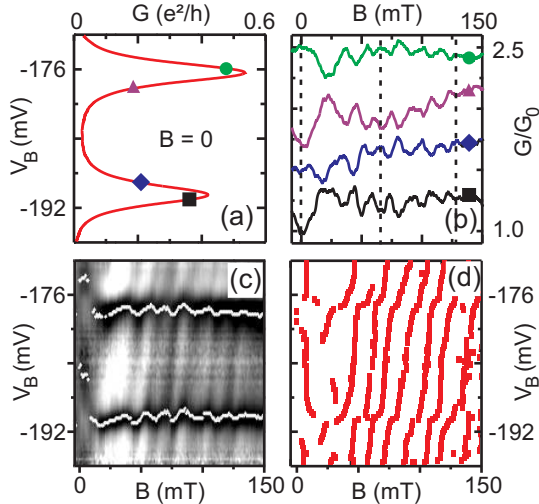


FIG. 4: (a) The  $N = 5$ -Kondo valley at a lower tunnel coupling  $V_A = -150$  mV and  $B = 0$ .  $\blacksquare, \blacklozenge, \bullet, \blacktriangle$  mark the gate voltages for the Aharonov-Bohm measurements shown in (b). (b) Normalized conductance  $G/G_0$  of the quantum ring in function of magnetic field  $B$ . The curves are offset for clarity. (c)  $G/G_0(B, V_B)$  as grey scale plot with Coulomb peak positions marked by white dots. (d) Position of the Aharonov-Bohm maxima extracted from (c).

Coulomb-blockade peak position indicates a change of the ground state. According to the theoretical calculation of Niemelä *et al.* [9] the transition period  $\Delta B$  is related to the number of electrons on the ring.  $\Delta B$  should be shortened by a factor of five for five electrons. In fair agreement, we observe a period of  $\Delta B \sim 13$  mT which is four to five times shorter compared to the open regime. The deviations from perfect periodicity especially at small magnetic fields have to be explained by the influence of some residual disorder.

We utilize the Kondo effect with its finite conductance to study the evolution of the Aharonov-Bohm maxima in the Coulomb-blockade valley. Fig. 4(d) shows the position of each maximum extracted from Fig. 4(c). At the Coulomb-blockade peak between  $V_B = -191$  mV and  $V_B = -189$  mV we observe a phase jump of  $\pi$ , indicated by the small kink visible for all magnetic fields. This is verified in Fig. 4(b): the conductance at  $B = 0$  changes from a minimum to a maximum. A second phase jump occurs at the next Coulomb-blockade resonance between  $V_B = -178$  mV and  $V_B = -176$  mV.

In the Coulomb valley the maxima show a smooth shift (Fig. 4(d)). These linear shifts appear in our two-terminal measurement only at finite magnetic field when the ring is threaded by at least half a flux quantum. Linear shifts of *normal* Aharonov-Bohm oscillations were recently reported by Ji *et al.* for a quantum dot in the Kondo regime embedded in an Aharonov-Bohm interferometer [17]. Their four-terminal measurement is interpreted in terms of smooth phase shifts by  $\pi$  across a Kondo resonance. In contrast we investigate a Kondo resonance far from the unitary limit in a quantum dot which itself

serves as the interferometer.

The exact mechanism for the observed linear shift of the Aharonov-Bohm maxima is still to be clarified, but it might be connected to the fact that the level structure of our small ring interferometer is influenced by the gate voltage. For a detailed understanding further theoretical work is necessary.

In conclusion, a small tuneable quantum ring with less than ten electrons is shown to exhibit Aharonov-Bohm oscillations as well as Coulomb-blockade. At strong coupling to the leads we find evidence of a Kondo effect induced by a single spin on the ring. The energy spectrum is strongly influenced by electron-electron interaction. An analysis of the phase evolution of the Aharonov-Bohm effect in the Kondo regime yields phase jumps by  $\pi$  at the Coulomb-blockade resonances and a smooth shift of the Aharonov-Bohm maxima in between.

We acknowledge discussions with S. Ulloa and J. König and financial support by BMBF, DIP and TMR.

\* Electronic address: keyser@nano.uni-hannover.de

- [1] L. P. Kouwenhoven, in *Mesoscopic Electron Transport*, edited by L. L. Sohn, L. P. Kouwenhoven, and G. Schön, NATO ASI Series (Kluwer, Dordrecht, 1997), vol. 345.
- [2] Y. Aharonov and D. Bohm, Phys. Rev. **115**, 485 (1959).
- [3] A. Lorke *et al.*, Phys. Rev. Lett. **84**, 2223 (2000).
- [4] R. J. Warburton *et al.*, Nature **405**, 926 (2000).
- [5] M. Ishii and K. Mastumoto, Jpn. J. Appl. Phys. **34**, 1329 (1995).
- [6] A. Fuhrer *et al.*, Nature **413**, 385 (2001).
- [7] U. F. Keyser *et al.*, Semicon. Sci. Technol. **17**, L22 (2002).
- [8] W.-C. Tan and J. C. Inkson, Semicon. Sci. Technol. **11**, 1635 (1996).
- [9] K. Niemelä *et al.*, Europhysics Letters **36**, 36 (1996).
- [10] J. Kondo, Progr. Theor. Phys. **32**, 37 (1964).
- [11] T. K. Ng and P. A. Lee, Phys. Rev. Lett. **61**, 1768 (1988).
- [12] L. I. Glazman and M. E. Raikh, JETP Lett. **47**, 452 (1988).
- [13] D. Goldhaber-Gordon *et al.*, Nature **391**, 156 (1998).
- [14] S. M. Cronenwett, T. H. Oosterkamp, and L. P. Kouwenhoven, Science **281**, 540 (1998).
- [15] J. Schmid *et al.*, Physica B **256**, 182 (1998).
- [16] F. Simmel *et al.*, Phys. Rev. Lett. **83**, 804 (1999).
- [17] Y. Ji, M. Heiblum, and H. Shtrikman, Phys. Rev. Lett. **88**, 076601 (2002).
- [18] Y. Ji *et al.*, Science **290**, 779 (2000).
- [19] U. F. Keyser *et al.*, Appl. Phys. Lett. **76**, 457 (2000).
- [20] S. Tarucha *et al.*, Phys. Rev. Lett. **77**, 3613 (1996).
- [21] J. Schmid *et al.*, Phys. Rev. Lett. **84**, 5824 (2000).
- [22] D. Sprinzak *et al.*, Phys. Rev. Lett. **88**, 176805 (2002).
- [23] P. L. McEuen *et al.*, Phys. Rev. B **45**, 11419 (1992).
- [24] M. Ciorga *et al.*, Phys. Rev. B **61**, 16315 (2000).
- [25] Y. Meir, N. S. Wingreen, and P. A. Lee, Phys. Rev. Lett. **70**, 2601 (1993).
- [26] J. Nygård, D. H. Cobden, and P. E. Lindelof, Nature **408**, 342 (2000).
- [27] D. Goldhaber-Gordon *et al.*, Phys. Rev. Lett. **81**, 5225 (1998).